Accurate conservative phase-field method for simulation of two-phase flows

By S. S. Jain

1. Motivation and objectives

Two-phase flows are ubiquitous in nature and have applications in engineering and natural processes such as atomization of jets and sprays, breaking waves, emulsions, boiling phenomena, carbon sequestration, and bubbly flows in cooling towers of nuclear power plants. Numerous challenges are associated with the numerical modeling of two-phase flows, primarily due to the presence of discontinuities at the interface and the inherent multiscale nature of the problem.

Over the years, many interface-capturing and interface-tracking methods have been proposed. The interface-capturing methods are preferred over interface-tracking methods due to the capability of the interface-capturing methods to handle dynamic topological changes implicitly. These methods can be broadly classified into a volume-of-fluid (VOF) method, a level-set (LS) method, a phase-field (PF) method, and hybrid methods such as a CLSVOF (coupled level-set and volume-of-fluid) method, and a VOSET (coupled volume-of-fluid and level-set) method, where typically two methods are combined to have the advantages of both methods (Mirjalili *et al.* 2017).

The VOF and LS methods are sharp-interface methods and are generally known to be accurate in representing the material interface, which is physically sharp in the continuum limit. The main disadvantages of these methods are that a VOF method involves an interface-reconstruction step that is complex and expensive, and an LS method is not conservative. The hybrid methods were proposed to overcome some of these challenges and combine the advantages of two methods, but they are known to be more complicated than the original methods. A PF method, in contrast, is a diffuse-interface approach that is relatively less expensive and simple to implement. Some PF models are also inherently conservative. Hence, we adopt a diffuse-interface approach in this work, and propose a novel PF method that is conservative and more accurate than some existing PF methods in the literature.

2. Phase-field method

2.1. *Cahn-Hilliard and Allen-Cahn models*

The classical PF methods are based on Cahn-Hilliard and Allen-Cahn equations (Cahn & Hilliard 1958; Allen & Cahn 1979) that were originally developed to model the phase separation and coarsening phenomena in solids and the motion of antiphase boundaries in crystalline solids, respectively. More recently, these methods have been adopted for modeling the interface between two fluids (Anderson *et al.* 1998). A Cahn-Hilliard PF model is conservative but involves a fourth-order spatial derivative in the equation, which requires careful construction of the numerical methods. In contrast, an Allen-Cahn PF model does not involve fourth-order derivatives in the equation, but is not conservative.

2.2. *Conservative phase-field model*

Starting from the Allen-Cahn equation, and subtracting the curvature-driven motion of the interface, Chiu & Lin (2011) derived a conservative diffuse-interface/phase-field (CDI/CPF) model for incompressible flows, which can be written as

$$\frac{\partial \phi}{\partial t} + \vec{\nabla} \cdot (\vec{u}\phi) = \vec{\nabla} \cdot \left\{ \Gamma \left[\epsilon \vec{\nabla}\phi - \phi(1-\phi) \frac{\vec{\nabla}\phi}{|\vec{\nabla}\phi|} \right] \right\}, \tag{2.1}$$

where ϕ is the PF variable which represents the volume fraction, $\vec{u}$ is the velocity, Γ represents the velocity-scale parameter, and ϵ is the interface thickness scale parameter. This model can be thought of as the one-step conservative LS method introduced by Olsson & Kreiss (2005), and is also sometimes referred to as a conservative/modified Allen-Cahn equation because it can be derived analytically starting from the Allen-Cahn equation. This model has since been widely used not only in the finite-volume/finite-difference setting but also in lattice-Boltzmann methods (Geier *et al.* 2015; Ren *et al.* 2016; Liang *et al.* 2018; Fakhari *et al.* 2018; Abadi *et al.* 2018; Aihara *et al.* 2019). Using central difference schemes, Mirjalili *et al.* (2020) showed that the PF variable, ϕ, remains bounded between 0 and 1 for incompressible flows, if the values for Γ and ϵ are appropriately chosen. More recently, Jain *et al.* (2020) proposed a CDI method for compressible flows and showed that ϕ remains bounded between 0 and 1 for compressible flows, with the use of central difference schemes, provided that an additional constraint on time-step size is satisfied. Additionally, Jain *et al.* (2020) showed that the transport of ϕ with this PF method also satisfies the total-variation diminishing (TVD) property. The compressible CDI model has been further coupled with a shock-capturing method for the simulation of high-Mach-number two-phase flows, extended to multiphase modeling of deforming solids, and also extended for higher-order explicit and compact central schemes by Jain *et al.* (2021).

This CDI/CPF method is easy to implement and cost-effective, but the two main issues with this model are (a) artificial distortion of the interface (alignment with the grid) and (b) limited accuracy. Jain *et al.* (2021) compared the compressible CDI method of Jain *et al.* (2020) with the quasi-conservative diffuse-interface method by Shukla *et al.* (2010) and Tiwari *et al.* (2013), and with the localized-artificial diffusivity based diffuse-interface method by Cook (2007) and Subramaniam *et al.* (2018) in the context of compressible flows and made the following conclusions. The CDI method is superior in maintaining the conservation property and in maintaining a constant interface thickness throughout the simulation, but it results in artificial distortion of the interface for long-time integrations and in the absence of surface tension effects. This behavior is, however, not limited to compressible flows and is valid for both incompressible and compressible flows. This alignment of the interface with the grid was also observed by Tiwari *et al.* (2013) with the quasi-conservative diffuse-interface method and by Wacławczyk (2015) and Chiodi & Desjardins (2017) in the context of a conservative level-set method. Note that, the exact amount of interface distortion is probably dependent on the choice of the numerical discretization. Some fixes proposed for this issue are to use a higher-order scheme (Tiwari *et al.* 2013; Jain *et al.* 2021) and the reformulation of the reinitialization procedure in the conservative LS method (Chiodi & Desjardins 2017).

To maintain the boundedness of ϕ with the CDI method, the criterion that needs to

be satisfied (Mirjalili *et al.* 2020; Jain *et al.* 2020) is

$$\Gamma^* \geq \frac{1}{(2\epsilon^* - 1)}, \tag{2.2}$$

where $\Gamma^* = \Gamma/|\vec{u}|_{max}$ and $\epsilon^* = \epsilon/(\Delta x)$ are the non-dimensionalized parameters. One way to improve the accuracy of a diffuse-interface method without increasing the grid resolution is by reducing ϵ, which improves the accuracy by making the interface sharper. But with the CDI method, as ϵ decreases, Γ needs to increase to keep ϕ bounded. For example, if ϵ is to be made smaller than one grid size (Δx), then $\Gamma > |\vec{u}|_{max}$. This increase in the value of Γ degrades the accuracy of the model and further increases the cost by imposing a more severe Courant-Friedrich-Lewy (CFL) restriction. Hence, the accuracy of the CDI model degrades as ϵ becomes small, particularly as ϵ approaches $0.5\Delta x$, which is not ideal. More recently, Chiu (2019) proposed an alternate model with a hope to obtain a model that is more accurate compared to the CDI model. But their proposed model was not conservative, and required solving two transport equations.

Being aware of all these issues associated with the PF methods in the literature, we therefore seek a method that is more accurate than the CDI method, is conservative, maintains boundedness of the volume fraction, converges (as ϵ decreases), is cost-effective, and is easy to implement and robust. With this objective, in this work, we propose a novel PF model, which we refer to as an accurate conservative diffuse-interface/phase-field (ACDI/ACPF) method, that has all the above-listed characteristics. Furthermore, following previous approaches (Abel *et al.* 2012; Raessi & Pitsch 2012; Chenadec & Pitsch 2013; Huang *et al.* 2020; Mirjalili & Mani 2021) we derive a consistent and conservative momentum transport equation for the proposed PF model, such that the resulting transport of momentum is consistent with the transport of the two-phase mixture mass and results in discrete kinetic energy conservation in the absence of dissipative mechanisms.

3. Proposed accurate conservative phase-field model

Ideally, we need the interface to be in an equilibrium state. This is achieved when the right-hand-side (RHS) terms in Eq. (2.1)—also called interface-regularization terms—are the stiffest terms. In this limit,

$$\vec{\nabla} \cdot \left[\epsilon \vec{\nabla}\phi - \phi(1-\phi)\vec{n}\right] = 0.$$

If s represents a coordinate along the interface normal, then the above equation can now be rewritten along this coordinate, with the normal $\vec{n} = \pm 1$, as

$$\frac{d^2\phi}{ds^2} \pm \frac{1}{\epsilon}\frac{d}{ds}\left[\phi(1-\phi)\right] = 0.$$

Choosing $\vec{n} = +1$, integrating the above relation, and using the conditions $\phi \to 0$ as $s \to -\infty$, we arrive at the relation

$$\frac{d\phi}{ds} = \frac{\phi(1-\phi)}{\epsilon}.$$

Further, let ψ represent the signed-distance function from the interface, such that ψ and s are related as $\psi(\phi) = s(\phi) - s(\phi = 0.5)$. With this, the above relation can be re-expressed in terms of ψ as

$$\frac{d\phi}{d\psi} = \frac{\phi(1-\phi)}{\epsilon}. \tag{3.1}$$

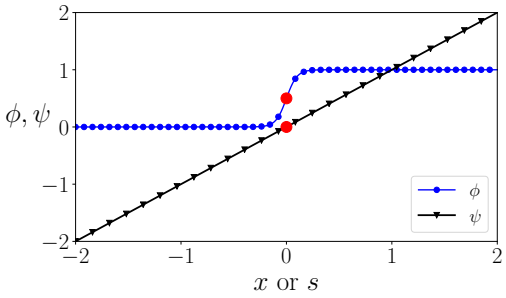

FIGURE 1. An illustration of the PF variable, ϕ, and the signed-distance function, ψ, for an interface located at $x = 0$. The two large dots are marked on the plots at $\phi = 0.5$ and $\psi = 0$, representing the location of the interface.

Now, integrating this relation and using the conditions $\phi = 0.5$ at $\psi = 0$, we arrive at the equilibrium kernel function for ϕ in terms of the signed-distance function ψ as

$$\phi = \frac{e^{(\psi/\epsilon)}}{1 + e^{(\psi/\epsilon)}} = \frac{1}{2}\left[1 + \tanh\left(\frac{\psi}{2\epsilon}\right)\right]. \tag{3.2}$$

To illustrate, a plot of ϕ and ψ, along s, is shown in Figure 1 for an interface located at $x = 0$. Now, using the relations in Eqs. (3.1)-(3.2), we can arrive at the relation

$$\phi(1-\phi) = \frac{1}{4}\left[1 - \tanh^2\left(\frac{\psi}{2\epsilon}\right)\right]. \tag{3.3}$$

Further, we can also show that the normal can be reexpressed in terms of ψ as

$$\vec{n} = \frac{\vec{\nabla}\phi}{|\vec{\nabla}\phi|} = \frac{\vec{\nabla}\psi}{|\vec{\nabla}\psi|}. \tag{3.4}$$

Similar relations were used by Wacławczyk (2015), Chiodi & Desjardins (2017), and Chiu (2019) to reformulate interface-capturing methods. Using the relation in Eq. (3.3), we replace the non-linear sharpening flux term $\phi(1-\phi)$ in Eq. (2.1) with the expression in terms of ψ. As shown in Figure 1, ψ is a better-behaved function compared with ϕ that does not contain any jumps/discontinuities. Hence, using ψ to compute the non-linear sharpening flux will result in more accurate discrete representation of the flux. Furthermore, with the same reasoning, we also replace the computation of the normal term $\vec{\nabla}\phi/|\vec{\nabla}\phi|$ in Eq. (2.1) with the expression in terms of ψ in Eq. (3.4). With these modifications, the proposed new PF model, an ACDI/ACPF method, can be written as

$$\frac{\partial \phi}{\partial t} + \vec{\nabla}\cdot(\vec{u}\phi) = \vec{\nabla}\cdot\left\{\Gamma\left\{\epsilon\vec{\nabla}\phi - \frac{1}{4}\left[1 - \tanh^2\left(\frac{\psi}{2\epsilon}\right)\right]\frac{\vec{\nabla}\psi}{|\vec{\nabla}\psi|}\right\}\right\}. \tag{3.5}$$

Not only is this form of the PF model derived to obtain a method that is more accurate than the CDI method, but also the terms in the model are carefully constructed such that the model also results in the transport of ϕ that is always bounded between 0 and 1 (see Section 3.2). For example, the diffusion term in the proposed ACDI model in Eq. (3.5) is still written in terms of ϕ, and we do not replace this with an equivalent expression for ψ. This is because, in the limit of $\phi \to 0$ *or* 1, the diffusion term that is expressed in terms of ψ could switch signs due to the error in the computation of ψ. This will result

in failure of the method to maintain a bounded ϕ between 0 and 1, and can potentially make the method non-robust.

All the terms in the proposed model are in divergence form, and hence, the model is conservative. The proposed model is also cost-effective and easy to implement because it requires solving a single scalar partial-differential equation. Additionally, the superior robustness and the convergence (with ϵ) properties of the model will be illustrated below.

3.1. *Calculation of* ψ

The proposed PF model requires the computation of ψ, and this can be easily calculated using the algebraic relation

$$\psi = \epsilon \ln\left(\frac{\phi + \varepsilon}{1 - \phi + \varepsilon}\right), \tag{3.6}$$

which is obtained by rearranging the relation in Eq. (3.2). Here, ε is a small number that is added, to both the numerator and the denominator, to avoid ψ going to $-\infty$ or ∞ when ϕ goes to 0 or 1, respectively (a value of $\varepsilon = 10^{-100}$ is used in this work). Additionally, if ϕ assumes values outside the range $[0, 1]$, the computation of ψ using the relation in Eq. (3.6) results in physically unrealizable values. But, because ϕ is always guaranteed to be bounded between 0 and 1, with the proposed PF model, the direct computation of ψ using Eq. (3.6) will not be an issue. Note that, ψ is only an approximation to a signed-distance function and not a perfect signed-distance function because the interface is generally not in equilibrium (a hyperbolic tangent function) due to the velocity gradients in the flow which pushes the interface away from its equilibrium state. Hence, it is not assumed, anywhere in this work, that ψ is a signed-distance function, e.g., for the computation of normal using Eq. (3.4), $|\vec{\nabla}\psi|$ is not set to 1.

3.2. *Choosing the parameters* Γ *and* ϵ

The values of Γ and ϵ are chosen such that the transport of ϕ is always bounded between 0 and 1. The criterion that needs to be satisfied is

$$\Gamma \geq |\vec{u}|_{max} \text{ and } \epsilon > 0.5\Delta x, \tag{3.7}$$

where $|\vec{u}|_{max}$ is the maximum value of the absolute velocity in the domain, and Δx is the grid-cell size. The derivation and proof of this criterion along with the associated verification simulations are deferred to a future article.

It is almost always practical and preferable to choose the minimum possible values for Γ and ϵ that satisfy the criterion in Eq. (3.7). Choosing the value of Γ to be equal to $|\vec{u}|_{max}$ makes the RHS of Eq. (3.5) the stiffest term in the equation, which is required for the interface to maintain an equilibrium kernel shape—a hyperbolic tangent function—throughout the simulation. A higher value for Γ, although it forces the interface to assume the equilibrium kernel shape more quickly, makes the RHS term in Eq. (3.5) stiffer and imposes an additional CFL restriction. Choosing the value of ϵ to be approximately equal to $0.5\Delta x$ is also preferred, because this keeps the interface, which is resolved on the grid, as sharp as possible. Increasing ϵ increases the interface thickness and, hence, reduces the accuracy of the method.

3.3. *Cost estimates and accuracy*

The choice of parameters Γ and ϵ in a diffuse-interface method imposes a restriction on the time-step size due to the viscous CFL criterion, which can be expressed as

$$\Delta t_{max} \sim \frac{\Delta x^2}{\Gamma \epsilon}. \tag{3.8}$$

From the boundedness criterion, for the CDI method, in Eq. (2.2), as $\epsilon^* \to 0.5$, the required Γ^* goes to ∞. Because both the proposed ACDI method in Eq. (3.5) and the CDI method in Eq. (2.1) maintain boundedness of ϕ for the choice of $\Gamma^* = 1$ and $\epsilon^* = 1$, the cost of both the CDI and the ACDI methods in terms of the required number of time steps is the same. But because the resolved interface becomes sharper as ϵ reduces, we are interested in estimating the cost of these methods for $\epsilon^* < 1$.

Using the boundedness criterion in Eq. (3.7) and expressing Δt_{max} in terms of ϵ^*, for the proposed ACDI method, the restriction on the time-step size is

$$\Delta t_{max} \sim \frac{\Delta x}{|\vec{u}|_{max}\epsilon^*}.$$

If ϵ^* is chosen to be equal to 0.55, then $\Delta t_{max}|_{\epsilon^*=0.55} = 20/11\ \Delta t_{max}|_{\epsilon^*=1}$, and $N_{\epsilon^*=0.55} = 0.55N_{\epsilon^*=1}$, where N is the number of time steps. Therefore, the cost is 1.8 times lower than that of the simulation with $\epsilon^* = 1$. Similarly, if $\epsilon^* = 0.51$, then the cost is 1.96 times lower. In contrast, for the CDI method, Δt_{max} can be expressed in terms of ϵ^* as

$$\Delta t_{max} \sim \frac{\Delta x}{|\vec{u}|_{max}} \left(2 - \frac{1}{\epsilon^*}\right).$$

If ϵ^* is chosen to be equal to 0.55, then $\Delta t_{max}|_{\epsilon^*=0.55} = 20/11\ \Delta t_{max}|_{\epsilon^*=1}$, and $N_{\epsilon^*=0.55} = 5.5N_{\epsilon^*=1}$. Therefore, the cost is 5.5 times higher than that of the simulation with $\epsilon^* = 1$. Similarly, if $\epsilon^* = 0.51$, then the cost is 25.5 times higher. Hence, with the proposed ACDI method, reducing ϵ not only makes the interface more sharp, but also reduces the cost of the simulation. In contrast, with the CDI method, the cost of the simulation increases as ϵ reduces. As $\epsilon^* \to 0.5$, the CDI method becomes prohibitively expensive.

Apart from the cost, reducing ϵ also increases the accuracy of the proposed ACDI method by making the resolved interface sharper. In contrast, for the CDI method, reducing ϵ, particularly for the values of $\epsilon^* < 1$, reduces the accuracy of the method, albeit making the interface sharper. This is because a value of $\epsilon^* < 1$ requires $\Gamma^* > 1$, which makes the RHS term in Eq. (2.1) stiffer. This increases the error associated with the calculation of the non-linear flux and the normal (as described in Section 3) and, therefore, exacerbates the issue of artificial interface distortion that was observed by Tiwari *et al.* (2013) and Jain *et al.* (2021). A quantitative comparison of the accuracy of the ACDI and CDI methods, with reducing ϵ, is presented in Section 6.1.1.

3.4. *Improvements in computation of surface tension force*

Surface tension force can be modeled as a stress or a body force. These are called integral and volumetric formulations, respectively. It is crucial to have a discrete balance between the surface tension force and the pressure terms to minimize the spurious currents around the interface (Francois *et al.* 2006). The continuum-surface force (CSF) formulation (Brackbill *et al.* 1992) is used in this work because it is easy to attain this balance with this formulation.

For a diffuse-interface method, the CSF formulation can be written as $\vec{F} = \sigma\kappa\vec{\nabla}\phi$, where κ is the curvature, and can be calculated as

$$\kappa = -\vec{\nabla} \cdot \vec{n} = -\vec{\nabla} \cdot \left(\frac{\vec{\nabla}\phi}{|\vec{\nabla}\phi|}\right). \tag{3.9}$$

It is known that the error associated with the computation of curvature is the primary reason for the formation of spurious currents (Popinet 2018). With the proposed ACDI

method, we now have access to the well-behaved, signed-distance function ψ. Hence, utilizing the relation in Eq. (3.4), curvature can instead be calculated as

$$\kappa = -\vec{\nabla} \cdot \vec{n} = -\vec{\nabla} \cdot \left(\frac{\vec{\nabla}\psi}{|\vec{\nabla}\psi|} \right), \tag{3.10}$$

which reduces the truncation errors in computation of κ and, therefore, the amount of spurious currents.

4. Coupling with incompressible Navier-Stokes equations

When an interface-capturing method is coupled with the Navier-Stokes equations, it is important to solve a form of the momentum equation that transports momentum consistently with the transport of mass. This is required to make the resulting coupled system robust in the limit of high-density ratio and high-Re flows.

If we represent the diffusion and sharpening fluxes on the RHS of Eq. (3.5), for phase l, as

$$\vec{a}_l = \Gamma \left\{ \epsilon \vec{\nabla}\phi_l - \frac{1}{4} \left[1 - \tanh^2 \left(\frac{\psi}{2\epsilon} \right) \right] \frac{\vec{\nabla}\psi}{|\vec{\nabla}\psi|} \right\}, \tag{4.1}$$

where ϕ_l is the volume fraction of phase l, then this relation satisfies the condition

$$\sum_{l=1}^{2} \vec{a}_l = 0. \tag{4.2}$$

The implied mass transport equation for the proposed ACDI method can then be written as

$$\frac{\partial \rho}{\partial t} + \vec{\nabla} \cdot (\vec{u}\rho) = \vec{\nabla} \cdot \vec{f}, \tag{4.3}$$

where

$$\vec{f} = \sum_{l=1}^{2} \rho_l \vec{a}_l = \left\{ (\rho_1 - \rho_2)\Gamma \left\{ \epsilon \vec{\nabla}\phi_1 - \frac{1}{4} \left[1 - \tanh^2 \left(\frac{\psi}{2\epsilon} \right) \right] \frac{\vec{\nabla}\psi}{|\vec{\nabla}\psi|} \right\} \right\}.$$

4.1. *Consistent momentum transport equation*

The consistency corrections for the momentum equation for the proposed ACDI method can be derived with the premise that a consistent momentum transport equation does not spuriously contribute to the kinetic energy of the system. The full coupled system of equations for the simulation of incompressible two-phase flows can then be written as

$$\frac{\partial \phi_1}{\partial t} + \vec{\nabla} \cdot (\vec{u}\phi_1) = \vec{\nabla} \cdot \vec{a}_1, \tag{4.4}$$

$$\frac{\partial \rho \vec{u}}{\partial t} + \vec{\nabla} \cdot (\rho \vec{u} \otimes \vec{u} + p\mathbb{1}) = \vec{\nabla} \cdot \underline{\underline{\tau}} + \vec{\nabla} \cdot (\vec{f} \otimes \vec{u}) + \sigma\kappa\vec{\nabla}\phi_1 + \rho\vec{g}, \tag{4.5}$$

$$\vec{\nabla} \cdot \vec{u} = 0, \tag{4.6}$$

where $\underline{\underline{\tau}}$ is the stress tensor, and $\vec{g}$ represents a generic body force. A fractional-step method (Kim & Moin 1985) is used to compute the pressure, which closes the system of equations. The resulting kinetic energy transport equation can be written as

$$\frac{\partial \rho k}{\partial t} + \vec{\nabla} \cdot (\rho \vec{u} k) + \vec{\nabla} \cdot (\vec{u}p) = \vec{\nabla} \cdot (\vec{f}k), \tag{4.7}$$

where all the terms are in conservative form. Thus, the proposed consistent momentum equation [Eq. (4.5)] results in conservation of total kinetic energy.

5. Numerical method: skew-symmetric-like splitting

In this work, the equations are discretized on an Eulerian Cartesian grid. A fourth-order Runge-Kutta method is used for time discretization, and a second-order flux-split conservative finite-difference/finite-volume central scheme is used for the spatial discretization of the equations.

The semi-discrete representation of the proposed ACDI PF model in Eq. (3.5) can be written as

$$\frac{\partial \phi}{\partial t} + \frac{\hat{\Phi}_j|_{(m+\frac{1}{2})} - \hat{\Phi}_j|_{(m-\frac{1}{2})}}{\Delta x_j} - \frac{\hat{A}_j|_{(m+\frac{1}{2})} - \hat{A}_j|_{(m-\frac{1}{2})}}{\Delta x_j} = 0, \tag{5.1}$$

where $\hat{\Phi}_j|_{(m\pm1/2)}$ and $\hat{A}_j|_{(m\pm1/2)}$ are the numerical fluxes for the convective and the interface-regularization (RHS) terms, respectively; the subscript m denotes the grid-cell index; and Δx_j represents the grid-cell size. Now, adopting the flux-splitting procedure for the interface regularization terms from Jain & Moin (2020), these numerical fluxes can be expressed as

$$\begin{aligned}
\hat{\Phi}_j|_{(m\pm\frac{1}{2})} &= \overline{\phi}^{(m\pm\frac{1}{2})}\overline{u}_j^{(m\pm\frac{1}{2})}, \\
\hat{A}_j|_{(m\pm\frac{1}{2})} &= \left\{ \Gamma \left\{ \frac{\epsilon}{\Delta x_j}\left(\Delta_j \phi\right) - \frac{1}{4}\left[1 - \tanh^2\left(\frac{\overline{\psi}^{(m\pm\frac{1}{2})}}{2\epsilon} \right) \right] \frac{\overline{\vec{\nabla}\psi}^{(m\pm\frac{1}{2})}}{|\vec{\nabla}\psi|} \right\} \right\},
\end{aligned} \tag{5.2}$$

where the overbar denotes an arithmetic average of the quantity evaluated at m and $m\pm1$; $\Delta_j\phi$ represents a difference along the jth coordinate as $\Delta_j\phi = \phi|_{(m+1)} - \phi|_m$. For the discrete representation of the consistent regularization terms in the mass, momentum, and energy equations, the same formulation in Eq. (5.2) should be used to maintain consistency. A skew-symmetric-like split scheme is used here, because these schemes result in reduced aliasing errors (Blaisdell *et al.* 1996; Chow & Moin 2003; Kennedy & Gruber 2008) and are known to improve the conservation properties of the quadratic quantities (Kravchenko & Moin 1997). Moreover, the scheme in Eq. (5.2) is also responsible for the superior—a less restrictive—boundedness criterion in Section 3.2 of the proposed PF model.

For the incompressible formulation presented in Section 4, a staggered grid is used, where the velocities are stored at the staggered locations to avoid pressure checker boarding. The PF variable and the pressure are located at the cell center.

6. Results

In this section, the simulation results with the newly proposed ACDI method are presented. A two-dimensional interface advection test case is presented in Section 6.1, where the proposed ACDI method and the CDI methods are compared in terms of accuracy. More importantly, the effect of reducing ϵ on the convergence behavior and the accuracy of the methods are discussed in Section 6.1.1. This is followed by the incompressible hydrodynamics-coupled simulations in Section 6.2, where the robustness of the proposed method is illustrated using the high-density-ratio droplet-laden isotropic turbulence simulation at infinite Re.

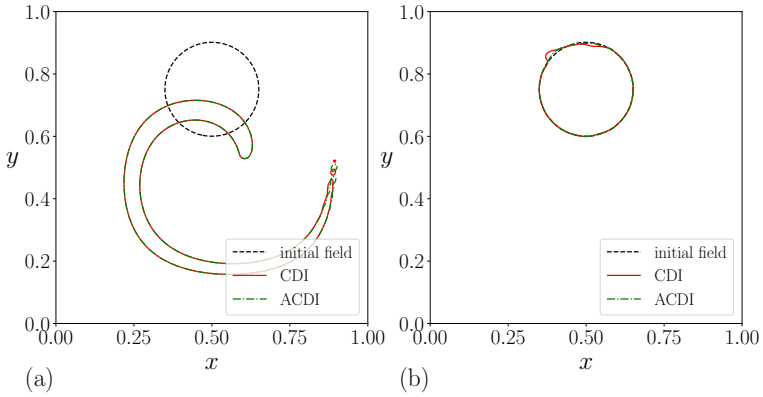

FIGURE 2. The shape of the drop at (a) half time of $t = 2$ and (b) final time of $t = 4$ in a shearing flow, computed in a domain discretized with a grid of size 256^2.

To quantitatively compare the error of the proposed ACDI method with that of the CDI method, we use the error, E, defined as

$$E = \int_\Omega |\phi_f - \phi_o| dV = \sum_m \Big| \phi_f|_m - \phi_o|_m \Big| dV, \tag{6.1}$$

where the subscripts f and o denote that the quantities are evaluated at the final and initial times, respectively.

6.1. *Drop in a shear flow*

This is a classical interface advection test case that was introduced by Bell *et al.* (1989) and Rider & Kothe (1998) and has been extensively used in the literature (Tryggvason *et al.* 2011) to assess the accuracy of the interface-capturing methods. In this test case, a circular drop/bubble of radius $R = 0.15$ is initially placed in the unit-sized domain at $(0.5, 0.75)$. A shearing velocity field given by

$$\begin{aligned} u &= -\sin^2(\pi x)\sin(2\pi y)\cos\left(\frac{\pi t}{T}\right), \\ v &= -\sin(2\pi x)\sin^2(\pi y)\cos\left(\frac{\pi t}{T}\right) \end{aligned} \tag{6.2}$$

is prescribed, where $T = 4$ is the time period of the flow; t is the time coordinate; x and y are the spatial coordinates; and u and v are the velocity components along the x and y directions, respectively. The drop undergoes a shearing deformation until $t = T/2 = 2$, and then the flow field is reversed with the hope that the initial drop shape is recovered at the final time of $t = T = 4$. Figure 2 shows the shape of the drop at the half time of $t = 2$ and the final time of $t = 4$ for the ACDI and the CDI methods, computed on a grid of size 256^2. The ACDI method is more accurate in recovering the circular shape of the drop compared with the CDI method. The error E computed using Eq. (6.1) for the ACDI method is 8.66×10^{-4} and for the CDI method is 1.95×10^{-3}.

6.1.1. *Effect of choice of ϵ on the accuracy of the method*

As described in Sections 3.2-3.3, it is important to use as small a value for ϵ as possible, while maintaining the boundedness of ϕ, because this makes the resolved interface more

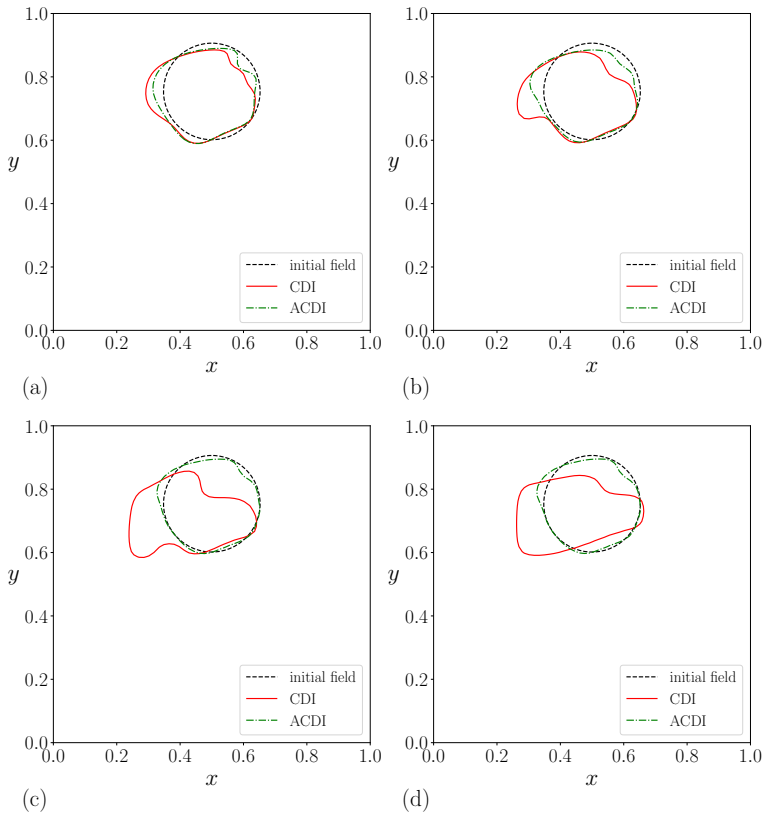

FIGURE 3. The final shape of the drop at $t = 4$ for (a) $\epsilon/\Delta x = 1$, (b) $\epsilon/\Delta x = 0.75$, (c) $\epsilon/\Delta x = 0.55$, and (d) $\epsilon/\Delta x = 0.51$, in a shearing flow computed with 64^2 grid points.

sharp. Section 3.3 showed that reducing the value of $\epsilon/\Delta x$ from 1 to 0.5 makes the simulation less expensive for the proposed ACDI method by increasing the maximum allowable time-step size, whereas reducing ϵ increases the cost for CDI method. In this section, the effect of varying the value of ϵ on the accuracy of the methods is evaluated.

Here, the test case of a drop in a shear flow from Section 6.1 is repeated, on a coarser grid of size 64^2, for various values of ϵ, and the shape of the drop that is recovered at the final time of $t = 4$ is shown in Figure 3. For the proposed ACDI method, the final drop shape is more circular, and it approaches the ideal shape, as the value of ϵ is reduced. But for the CDI method, the final drop shape is more distorted as the value of ϵ is reduced. Furthermore, the error E is plotted against different values of ϵ in Figure 4. The error for the proposed ACDI method decreases as $\epsilon/\Delta x$ decreases, all the way up to $\epsilon/\Delta x = 0.5$. But the error for the CDI method increases as $\epsilon/\Delta x$ decreases for $\epsilon/\Delta x < 1$. Hence, the proposed ACDI method not only becomes less expensive as $\epsilon/\Delta x$ decreases, but also becomes more accurate; therefore, the method converges with decreasing $\epsilon/\Delta x$. The CDI method, in contrast, not only becomes more expensive as $\epsilon/\Delta x$ decreases but also becomes less accurate; therefore, the method diverges with decreasing $\epsilon/\Delta x$.

6.2. *Droplet-laden isotropic turbulence*

In this section, the simulation of a droplet-laden isotropic turbulence is presented on coarse grids. It is well known that the coarse-grid simulation of a turbulent flow is a

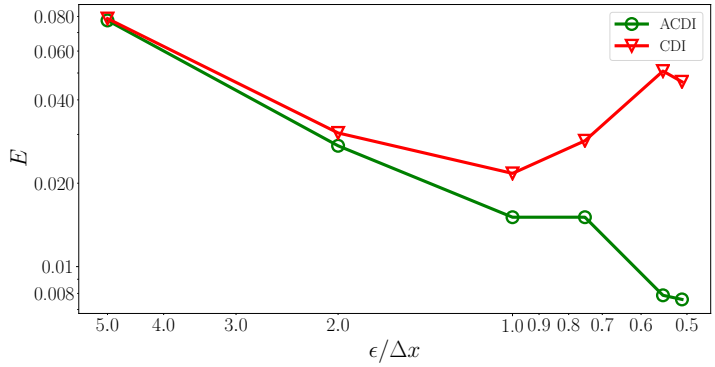

FIGURE 4. Comparison of the error, E, computed using Eq. (6.1), at the final time of $t = 4$ for the CDI and ACDI methods. The test case is the drop in a shear flow, computed in a domain discretized with a grid of size 64^2.

good test of the nonlinear stability and robustness of the method, which were previously studied, for single-phase flows, by Honein & Moin (2004), Mahesh *et al.* (2004), Hou & Mahesh (2005), and Subbareddy & Candler (2009), and for two-phase flows by Jain & Moin (2020). This is due to the lack of grid resolution to support dissipative mechanisms that stabilize the method. Here, high-density-ratio droplet-laden isotropic turbulence is simulated at finite and infinite Re. The infinite-Re simulation corresponds to an inviscid case, where there are no dissipative mechanisms, and acts as a true test of robustness of the method.

For the infinite-Re simulation case, the proposed ACDI method is coupled with both the consistent momentum transport equation in Eq. (4.5), which results in discrete kinetic energy conservation, and the standard momentum equation (inconsistent), which does not conserve kinetic energy. This is done to illustrate the importance of solving the consistent momentum transport equation.

The initial setup consists of a single spherical drop, of radius $R = 1$, that is placed at the center of the triply periodic domain. The domain has dimensions of $2\pi \times 2\pi \times 2\pi$, and is discretized into a grid of size $64 \times 64 \times 64$. The velocity field is initialized using the energy spectrum

$$E(k) \propto k^4 \exp\left[-2\left(\frac{k}{k_o}\right)^2\right], \tag{6.3}$$

where k is the wavenumber, and k_o is the most energetic wavenumber. Here, k_o is chosen to be equal to 4, and hence, the initial Taylor microscale is set as $\lambda_o = 2/k_o = 0.5$.

The density of the droplet fluid is $\rho_1 = 1000$, and the density of the carrier fluid is $\rho_2 = 1$. The surface tension between the two fluids is set to zero; i.e., the Weber number is ∞. For the finite-Re simulation, the dynamic viscosity of the two fluids is chosen to be $\mu_1 = 1.732$ and $\mu_2 = 1.732 \times 10^{-3}$, such that the initial Taylor-scale Reynolds number is $Re_{\lambda,o} = 100$, where, the Taylor scale Reynolds number is defined as $Re_\lambda = u_{rms}\lambda/\nu$, where $u_{rms} =< u_i u_i > /3 = (2/3)\int_0^\infty E(k)dk$ is the root-mean-square velocity fluctuation. For the infinite-Re simulation, the dynamic viscosity of the two fluids is chosen to be $\mu_1 = \mu_2 = 0$, such that $Re_{\lambda,o} = \infty$.

The snapshots of the simulation results for the $Re_{\lambda,o} = 100$ case at time $t = 0$ and the final time of $t = 5.7735$ are presented in Figure 5. Note that the breakup of the droplets and ligaments seen in this case is induced by the lack of grid resolution and, therefore,

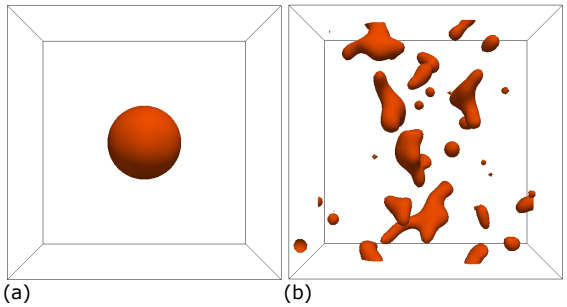

FIGURE 5. The snapshots from the droplet-laden isotropic turbulence simulation with the droplet-to-carrier fluid density ratio of $\rho_1/\rho_2 = 1000$, and the initial Taylor-scale Reynolds number of $Re_{\lambda,o} = 100$, at (a) $t = 0$ and (b) $t = 5.7735$.

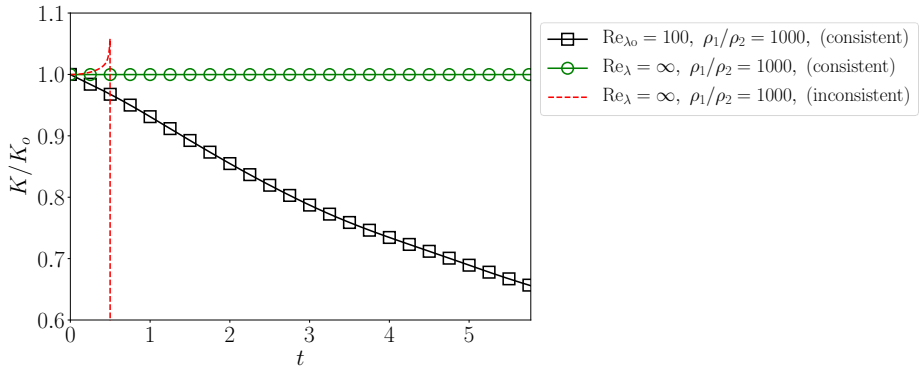

FIGURE 6. The evolution of total kinetic energy for the droplet-laden isotropic turbulence simulation for both finite and infinite Re. The consistent formulation is the PF model coupled with the proposed consistent momentum transport equation in Eq. (4.5), and the inconsistent formulation is the PF model coupled with the standard momentum equation.

should not be considered physical. One needs to implement a subgrid-scale model to correctly predict the behavior of droplet breakup and the drop-size distribution. Here, we are instead interested in testing the robustness of the proposed ACDI method and the consistent momentum transport equation.

The time evolution of the total kinetic energy $K = \rho u_i u_i/2$, normalized by the initial value, for both finite- and infinite-Re cases is shown in Figure 6. For the finite-Re case, the total kinetic energy of the system decays due to the viscous dissipation; and for the infinite-Re case, the kinetic energy is conserved throughout the simulation (as expected), which results in stable numerical simulations. For the infinite-Re case, results from the inconsistent momentum formulation are also shown in Figure 6 for comparison. Due to the inconsistent transport of momentum, the total kinetic energy is not conserved; therefore, the simulation diverges.

6.3. *Spurious currents in a stationary drop/bubble*

In this section, a simple test case of a stationary drop/bubble is used to evaluate the accuracy in computing surface tension force with the proposed ACDI method. The CSF formulation involves computation of curvature, and the error in computing curvature results in spurious currents. Hence, the maximum magnitude of spurious currents can be

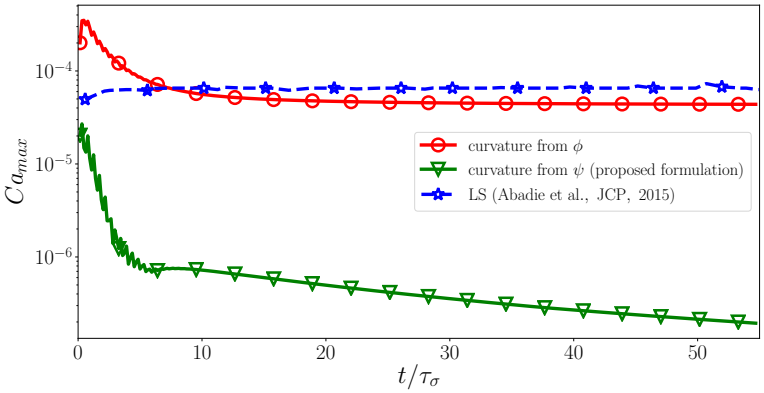

FIGURE 7. Evolution of the maximum non-dimensional spurious currents (Ca_{max}) with time. Time is normalized by the capillary time-scale $\tau_\sigma = \sqrt{\rho D^3/\sigma}$. LS denotes an LS method.

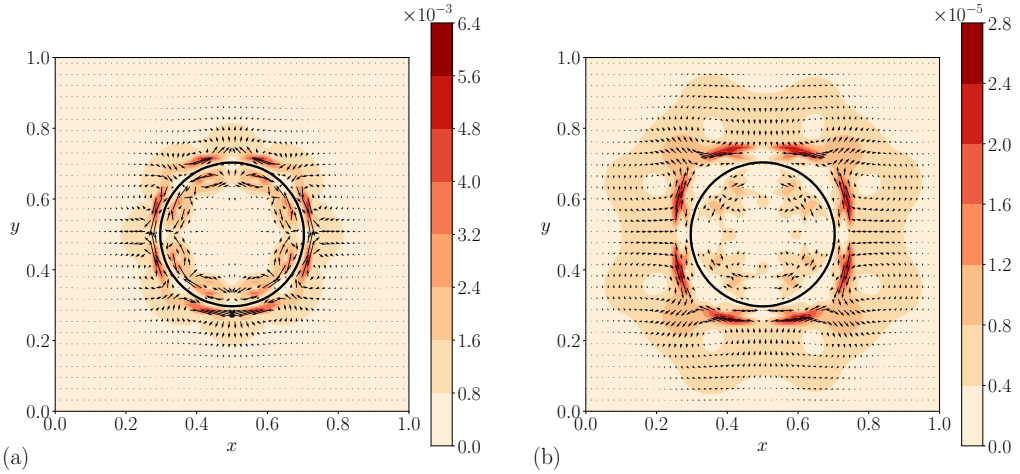

FIGURE 8. Form of the spurious currents around the interface at $t/\tau_\sigma \approx 55$ with curvature computed using (a) ϕ [Eq. (3.9)] and (b) ψ [Eq. (3.10)]. Here, the color represents the magnitude of the velocity in simulation units.

used as a metric to estimate the accuracy in the implementation of surface tension force terms.

A two-dimensional stationary drop of radius $R = 0.4$ is placed at the center of a square domain of unit size. The density and viscosity of the droplet fluid and the surrounding fluid are set to be equal. The fluid properties are chosen such that the Laplace number is $La = \rho D\sigma/\mu^2 = 12000$. The maximum magnitude of the non-dimensional spurious currents ($Ca_{max} = \mu|\vec{u}|_{max}/\sigma$, where Ca is the capillary number) in the domain is computed and plotted with time in Figure 7. A significant reduction in the spurious currents, by over 2 orders of magnitude, can be seen with the proposed ACDI method when the curvature is computed using Eq. (3.10), as opposed to Eq. (3.9).

Furthermore, to compare the present formulation with the LS formulation, the results from Abadie *et al.* (2015) are also presented in Figure 7. The curvature computation is very accurate in an LS method due to the use of a signed-distance function to compute

interface normals. Although the improved curvature computation results in improving the accuracy of the surface-tension force, the well-balanced nature of the surface tension model gets destroyed due to the reinitialization step in the LS method (Abadie *et al.* 2015). With the proposed ACDI method, the well-balanced nature of the surface tension model is retained, unlike the LS method, resulting in significantly lower magnitude of spurious currents compared with an LS method.

7. Conclusions

In this work, we propose a novel PF model for the simulation of two-phase flows that is accurate, conservative, bounded, and robust. The proposed model conserves the mass of each phase and results in bounded transport of the volume fraction. We present results from the canonical test cases of a drop in a shear flow, showing an improvement in accuracy over the commonly used conservative PF method. We further derive a consistent and conservative momentum transport equation for the proposed PF model that results in discrete conservation of kinetic energy, which is a sufficient condition for the numerical stability of incompressible flows in the absence of dissipative mechanisms.

We discretize the proposed PF model using the second-order flux-split conservative central scheme proposed by Jain & Moin (2020), which reduces the aliasing error and is also responsible for the superior boundedness property of the model. To illustrate the robustness of the method in simulating high-density-ratio turbulent two-phase flows, we present the numerical simulations of droplet-laden isotropic turbulence at infinite Reynolds numbers for a density ratio of 1000.

Acknowledgments

This investigation was supported by the Franklin P. and Caroline M. Johnson Graduate Fellowship.

REFERENCES

Abadi, R. H. H., Rahimian, M. H. & Fakhari, A. 2018 Conservative phase-field lattice-Boltzmann model for ternary fluids. *J. Comput. Phys.* **374**, 668–691.

Abadie, T., Aubin, J. & Legendre, D. 2015 On the combined effects of surface tension force calculation and interface advection on spurious currents within volume of fluid and level set frameworks. *J. Comput. Phys.* **297**, 611–636.

Abels, H., Garcke, H. and Grün, G. 2015 Thermodynamically consistent, frame indifferent diffuse interface models for incompressible two-phase flows with different densities. *Math. Models Methods Appl. Sci.* **22**, 1150013.

Aihara, S., Takaki, T. & Takada, N. 2019 Multi-phase-field modeling using a conservative Allen–Cahn equation for multiphase flow. *Comput. Fluids* **178**, 141–151.

Allen, S. M. & Cahn, J. W. 1979 A microscopic theory for antiphase boundary motion and its application to antiphase domain coarsening. *Acta Metall.* **27**, 1085–1095.

Anderson, D. M., McFadden, G. B. & Wheeler, A. A. 1998 Diffuse-interface methods in fluid mechanics. *Annu. Rev. Fluid Mech.* **30**, 139–165.

Bell, J. B., Colella, P. & Glaz, H. M. 1989 A second-order projection method for the incompressible Navier-Stokes equations. *J. Comput. Phys.* **85**, 257 – 283.

Blaisdell, G., Spyropoulos, E. & Qin, J. 1996 The effect of the formulation of

nonlinear terms on aliasing errors in spectral methods. *Appl. Numer. Math* **21**, 207–219.

Brackbill, J. U., Kothe, D. B. & Zemach, C. 1992 A continuum method for modeling surface tension. *J. Comput. Phys.* **100**, 335–354.

Cahn, J. W. & Hilliard, J. E. 1958 Free energy of a nonuniform system. i. Interfacial free energy. *J. Chem. Phys.* **28**, 258–267.

Chenadec, V. L. & Pitsch, H. 2013 A monotonicity preserving conservative sharp interface flow solver for high density ratio two-phase flows. *J. Comput. Phys.* **249**, 185–203.

Chiodi, R. & Desjardins, O. 2017 A reformulation of the conservative level set reinitialization equation for accurate and robust simulation of complex multiphase flows. *J. Comput. Phys.* **343**, 186–200.

Chiu, P.-H. 2019 A coupled phase field framework for solving incompressible two-phase flows. *J. Comput. Phys.* **392**, 115–140.

Chiu, P.-H. & Lin, Y.-T. 2011 A conservative phase field method for solving incompressible two-phase flows. *J. Comput. Phys.* **230**, 185–204.

Chow, F. K. & Moin, P. 2003 A further study of numerical errors in large-eddy simulations. *J. Comput. Phys.* **184**, 366–380.

Cook, A. W. 2007 Artificial fluid properties for large-eddy simulation of compressible turbulent mixing. *Phys. Fluids* **19**, 055103.

Fakhari, A., Li, Y., Bolster, D. & Christensen, K. T. 2018 A phase-field lattice Boltzmann model for simulating multiphase flows in porous media: Application and comparison to experiments of CO_2 sequestration at pore scale. *Adv. Water* **114**, 119–134.

Francois, M. M., Cummins, S. J., Dendy, E. D., Kothe, D. B., Sicilian, J. M. & Williams, M. W. 2006 A balanced-force algorithm for continuous and sharp interfacial surface tension models within a volume tracking framework. *J. Comput. Phys.* **213**, 141–173.

Geier, M., Fakhari, A. & Lee, T. 2015 Conservative phase-field lattice Boltzmann model for interface tracking equation. *Phys. Rev. E* **91**, 063309.

Honein, A. E. & Moin, P. 2004 Higher entropy conservation and numerical stability of compressible turbulence simulations. *J. Comput. Phys.* **201**, 531–545.

Hou, Y. & Mahesh, K. 2005 A robust, colocated, implicit algorithm for direct numerical simulation of compressible, turbulent flows. *J. Comput. Phys.* **205**, 205–221.

Huang, Z., Lin, G. & Ardekani, A. M. 2020*a* Consistent and conservative scheme for incompressible two-phase flows using the conservative Allen-Cahn model. *J. Comput. Phys.* **420**, 109718.

Jain, S. S., Adler, M. C., West, J. R., Mani, A., Moin, P. & Lele, S. K. 2021 Assessment of diffuse-interface methods for compressible multiphase fluid flows and elastic-plastic deformation in solids. *arXiv:2109.09729 [physics.comp-ph].* .

Jain, S. S., Mani, A. & Moin, P. 2020 A conservative diffuse-interface method for compressible two-phase flows. *J. Comput. Phys.* **418**, 109606.

Jain, S. S. & Moin, P. 2020 A kinetic energy and entropy preserving scheme for the simulation of compressible two-phase turbulent flows. *Annual Research Briefs,* Center for Turbulence Research, Stanford University, pp. 299-312.

Kennedy, C. A. & Gruber, A. 2008 Reduced aliasing formulations of the convective

terms within the Navier–Stokes equations for a compressible fluid. *J. Comput. Phys.* **227**, 1676–1700.

Kim, J. & Moin, P. 1985 Application of a fractional-step method to incompressible Navier-Stokes equations. *J. Comput. Phys.* **59**, 308–323.

Kravchenko, A. & Moin, P. 1997 On the effect of numerical errors in large eddy simulations of turbulent flows. *J. Comput. Phys.* **131**, 310–322.

Liang, H., Xu, J., Chen, J., Wang, H., Chai, Z. & Shi, B. 2018 Phase-field-based lattice Boltzmann modeling of large-density-ratio two-phase flows. *Phys. Rev. E* **97**, 033309.

Mahesh, K., Constantinescu, G. & Moin, P. 2004 A numerical method for large-eddy simulation in complex geometries. *J. Comput. Phys.* **197**, 215–240.

Mirjalili, S., Ivey, C. B. & Mani, A. 2020 A conservative diffuse interface method for two-phase flows with provable boundedness properties. *J. Comput. Phys.* **401**, 109006.

Mirjalili, S., Jain, S. S. & Dodd, M. 2017 Interface-capturing methods for two-phase flows: An overview and recent developments. *Annual Research Briefs,* Center for Turbulence Research, pp. 117–135.

Mirjalili, S. & Mani, A. 2021 Consistent, energy-conserving momentum transport for simulations of two-phase flows using the phase field equations. *J. Comput. Phys.* **426**, 109918.

Olsson, E. & Kreiss, G. 2005 A conservative level set method for two phase flow. *J. Comput. Phys.* **210**, 225–246.

Popinet, S. 2018 Numerical models of surface tension. *Annu. Rev. Fluid Mech.* **50**, 49–75.

Raessi, M. & Pitsch, H. 2012 Consistent mass and momentum transport for simulating incompressible flows with large density ratios using the level set method. *Comput. Fluids* **63**, 70–81.

Ren, F., Song, B., Sukop, M. C. & Hu, H. 2016 Improved lattice Boltzmann modeling of binary flow based on the conservative Allen-Cahn equation. *Phys. Rev. E* **94**, 023311.

Rider, W. J. & Kothe, D. B. 1998 Reconstructing volume tracking. *J. Comput. Phys.* **141**, 112–152.

Shukla, R. K., Pantano, C. & Freund, J. B. 2010 An interface capturing method for the simulation of multi-phase compressible flows. *J. Comput. Phys.* **229**, 7411–7439.

Subbareddy, P. K. & Candler, G. V. 2009 A fully discrete, kinetic energy consistent finite-volume scheme for compressible flows. *J. Comput. Phys.* **228**, 1347–1364.

Subramaniam, A., Ghaisas, N. S. & Lele, S. K. 2018 High-order Eulerian simulations of multimaterial elastic–plastic flow. *J. Fluids Eng.* **140**, 050904.

Tiwari, A., Freund, J. B. & Pantano, C. 2013 A diffuse interface model with immiscibility preservation. *J. Comput. Phys.* **252**, 290–309.

Tryggvason, G., Scardovelli, R. & Zaleski, S. 2011 *Direct Numerical Simulations of Gas–Liquid Multiphase Flows*. Cambridge University Press.

Wacławczyk, T. 2015 A consistent solution of the re-initialization equation in the conservative level-set method. *J. Comput. Phys.* **299**, 487–525.